

LONG RANGE FADING PREDICTION TO ENABLE ADAPTIVE TRANSMISSION AT ANOTHER CARRIER¹

Tung-Sheng Yang⁺, Alexandra Duel-Hallen⁺, and Hans Hallen^{*}

⁺North Carolina State University
Dept. of Electrical and Computer Engineering
Box 7911, Raleigh, NC 27695-7911
E-mail: {tsyang, sasha}@eos.ncsu.edu

^{*}North Carolina State University
Dept. of Physics
Raleigh, NC 27695-8202
E-mail: Hans_Hallen@eos.ncsu.edu

ABSTRACT

Adaptive transmission techniques usually require accurate channel estimation and feedback of channel state information. For fast vehicle speeds, reliable adaptive transmission also requires long range prediction of future Channel State Information (CSI) since the channel conditions are rapidly time-variant. In this paper, we propose to use past channel observations of one carrier to predict future CSI and perform adaptive modulation without feedback for another correlated carrier. We develop the minimum mean-square-error long range channel prediction algorithm that utilizes the time and frequency domain correlation function of the Rayleigh fading channel and a robust method that adapts to channel variations. Statistical model of the prediction error is used in the design of reliable adaptive modulation methods. We use a standard stationary fading channel model (the Jakes model) and a novel physical channel model to test our algorithm. Significant gains relative to non-adaptive techniques are demonstrated for sufficiently correlated channels and realistic prediction range.

1. INTRODUCTION

High speed wireless communications require robust channel estimation and adaptive transmission to satisfy the tremendous growth in demand for capacity. The idea of adaptive transmission [1-4] is to change the transmission parameters according to the instantaneous fading channel power without sacrificing bit-error rate (BER). For example, adaptive modulation methods can provide higher bit rates relative to conventional signaling by transmitting at high rate under favorable channel conditions, and reducing the throughput as the channel degrades. These adaptive modulation techniques depend on accurate channel state information (CSI) that can be acquired from different sources. If the communication between the two stations is bi-directional and the channel can be considered reciprocal, then each station can estimate the channel quality on the basis of the received symbols and adapt the parameters to this estimation. This is called open-loop adaptation [5]. If the channel is not reciprocal, the receiver has to estimate channel quality from feedback resulting in closed-loop adaptation. The feedback delay, overhead, and processing delay degrade the performance of adaptive modulation, especially in rapidly time

variant fading. Even in open-loop channels, current CSI is not sufficient since future channel conditions need to be known to adapt transmission parameters. To realize the potential of adaptive transmission methods, the channel variations have to be reliably predicted at least several milliseconds ahead.

Recently, a novel adaptive long-range prediction (LRP) method was proposed in [6-9]. This algorithm employs an autoregressive (AR) model to characterize the fading channel and computes the minimum mean-square-error (MMSE) estimate of a future fading coefficient based on a number of past observations. The advantage of this algorithm relative to conventional methods is due to its low sampling rate (on the order of twice the maximum Doppler shift and much lower than the data rate), which results in longer memory span and further prediction into the future for a fixed filter length. The accuracy of this algorithm is determined by the rate of change of amplitude, frequency and phase of each path [6,9,12,17]. However, the variation of these parameters is not captured by the standard Jakes model or a stationary random process description. To validate this long-range prediction algorithm, a novel physical channel modeling based on the method of images is proposed in [9,12,17].

In this paper, we extend the long-range prediction algorithm into frequency domain. In particular, we concentrate on the scenario where we observe a received uplink signal at the carrier frequency f^1 and attempt to predict the downlink signal at the carrier frequency f^2 without feedback from the mobile. Alternatively, a signal at frequency f^1 can be fed back and a signal at adjacent frequency f^2 is predicted without feedback. To accomplish this prediction, the predicted samples must be sufficiently correlated with the observations in both time and frequency. This technique can be applied in correlated uplink and downlink channels, in orthogonal frequency division multiplexing (OFDM) systems (where narrow correlated sub-channels are employed) or other wideband systems to reduce feedback and overhead requirements.

The remainder of this paper is organized as follows. In section 2, we present the system model and describe the theoretical MMSE long-range prediction, a robust prediction method and the statistical model of the prediction error. In section 3, the adaptive modulation scheme aided by the long-range prediction is discussed. Finally, section 4 presents computer simulation results to demonstrate the prediction range

¹ This research was supported by ARO grant DAA-19-01-1-0638.

in frequency domain. We extend the physical model to accommodate multiple carrier frequencies and use it to test the proposed channel prediction algorithm. We use this model to examine sensitivity of adaptive modulation performance to the variation of root mean square delay spread and identify typical and challenging situations encountered in practice.

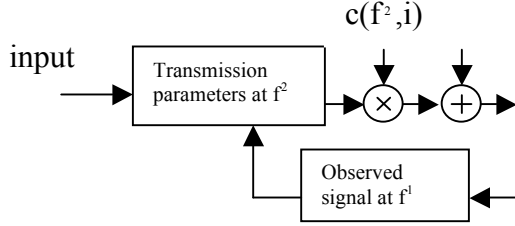


Fig. 1. System model

2. CHANNEL MODEL AND LONG RANGE PREDICTION

The statistics of fading signals received at correlated carriers are discussed in [10]. The fading coefficients at two frequencies f^1 and f^2 can be expressed as:

$$c(f^i, t) = \sum_{n=1}^N A_n e^{j(2\pi f_n t + \phi_n)}, \quad i=1,2 \quad (1)$$

where for the n^{th} path, A_n is the (real) amplitude and f_n is the Doppler shift. The phase difference of the n^{th} path $\phi_{2n} - \phi_{1n} = 2\pi\Delta f T_n$ where $\Delta f = f^2 - f^1$ is the frequency separation, and T_n is the excess propagation delay. For large N , $c(f^n, t)$ is distributed approximately as a zero mean complex Gaussian random variable. (We assume $E[|c(f^n, t)|^2] = 1$.) Hence the amplitudes $\alpha(f^1, t) = |c(f^1, t)|$ and $\alpha(f^2, t) = |c(f^2, t)|$ are both Rayleigh distributed. Assume angular distribution of the incident power is uniform between $[0, 2\pi]$, horizontal directivity pattern of the receiving antenna is 1, and the propagation delay T_n is exponentially distributed [10] with the probability density function (pdf) $p(T) = \frac{1}{\sigma} e^{-T/\sigma}$, where σ is a measure (rms delay spread [11]) of the time delay spread. The cross-correlation of the two fading signals with the time difference $\tau = |t_1 - t_2|$, maximum Doppler shift f_{dm} and the frequency separation $\Delta f = f^2 - f^1$ can be derived as [15]:

$$R(\tau, \Delta f) = E[c(f^1, t) c^*(f^2, t + \tau)] = R_r(\tau) R_f(\Delta f) \quad (2)$$

where $R_r(\tau) = J_0(2\pi f_{dm} \tau)$ is the zero order Bessel function and $R_f(\Delta f) = \frac{1}{1 + (2\pi\Delta f \sigma)^2} - j \frac{2\pi\Delta f \sigma}{1 + (2\pi\Delta f \sigma)^2}$.

To generate the signals, $c(f^1, t)$ was created first using the Jakes model [10] for given excess delay distribution. In this paper, we employ the 9 oscillators Jakes model with the maximum Doppler shift $f_{dm} = 100\text{Hz}$. Then $c(f^2, t)$ was generated from $c(f^1, t)$ using the same parameters except phases shifts as in (1). Using this fading model and a non-stationary physical model employed in Section 4, we characterize the capability of the proposed method to enable adaptive modulation.

The discrete-time system model is illustrated in Fig. 1. The frequency of observed CSI is f^1 and the frequency of transmitted signal is f^2 . Let $c(f^n, i)$, $n=1,2$, be samples of the fading signal $c(f^n, t)$ at the sampling interval T_s . Assume stationary and ergodic time-varying complex channel gain sequence $\alpha(f^n, i) = |c(f^n, i)|$ with distribution $p(x)$. The linear MMSE prediction of the future channel sample $c(f^2, n)$ at frequency f^2 based on p previously observed samples $c(f^1, n-j)$ at frequency f^1 is given by:

$$\hat{c}(f^2, n) = \sum_{j=1}^p d_j c(f^1, n-j) \quad (3)$$

The optimal coefficients d_j are determined as $\underline{d} = \mathbf{R}^{-1} \underline{r}$, where $\underline{d} = (d_1 \dots d_p)^T$. \mathbf{R} is the autocorrelation matrix ($p \times p$) with coefficients $R_{ij} = E[c^*(f^1, n-i) c(f^1, n-j)]$ and \underline{r} is the autocorrelation vector ($p \times 1$) with coefficients $r_j = E[c(f^2, n) c^*(f^1, n-j)]$. The resulting MMSE is given by

$$E[|e(n)|^2] = E[|c(f^2, n) - \hat{c}(f^2, n)|^2] = 1 - \sum_{j=1}^p d_j r_j. \quad \text{In practice, the}$$

samples $c(f^1, n)$ are observed in the presence of additive white Gaussian noise (AWGN) $z(i)$ with power spectrum density (PSD) N_0 . Equation (3) and the MMSE can be easily modified to include noisy observations [7]. As p increases, the MMSE saturation level is approached. With the knowledge of the cross-correlation function (2), we can derive the closed form expression of MMSE for $p = \infty$ and one-step prediction. Let $r(k)$ be the autocorrelation of the noisy fading channel samples $r(k) = E[(c(f^1, n-k) + z(n-k))(c(f^1, n) + z(n))^*] = R_n(k) + \delta(k)N_0$, where $R_n(k) = E[c(f^1, n-k) c^*(f^1, n)] = R_r(kT_s)$ is the discrete time autocorrelation function of the fading channel. Since $r(k)$ is a

correlation sequence, it can be represented as $r(k) = \sum_{j=-\infty}^0 r(j) r^+(k-j)$

where $r(k)$ and $r^+(k)$ are the sequences that satisfy $r(k) = 0$ when $n > 0$ and $r^+(k) = 0$ when $n < 0$. The MMSE can be expressed as [15,16]:

$$\text{MMSE} = R_n(0) - |R_r(\Delta f)|^2 [R_n(0) - r^+(0)^2 + N_0] \quad (4)$$

where $r^+(0)^2 = \exp\left\{\frac{1}{2\pi} \int_{-\infty}^{\infty} \ln[R_w(w) + N_0] dw\right\}$, and

$R_w(w) = \sum_{n=-\infty}^{\infty} R_n(n) e^{-jwn}$ is the folded power spectrum of the

channel. In Fig. 2, the theoretical MMSE of one-step prediction (4) vs. normalized frequency separation $\Delta f \sigma$ is plotted for different values of signal-to-noise ratio (SNR). The sampling rate $f_s = 5f_{dm}$ is chosen since it results in near optimal performance for LRP [7]. The prediction range is $0.2/f_{dm}$ seconds. We also compare the MMSE of the system with filter order $p = 100$ (see (3)). We found that for $p = 100$, the MMSE approaches the optimal case ($p = \infty$) for $f_s = 5f_{dm}$. Throughout the paper, we employ $p = 100$ and the sampling rate of 500Hz assuming the maximum Doppler shift of 100Hz. The observation interval of 100 samples is used to estimate the autocorrelation function in the algorithm above and to achieve convergence in the adaptive method described below. The SNR in the observations is chosen as 80dB. In practice, noise-reduction techniques can be employed to reduce the noise present in the observations [7,9].

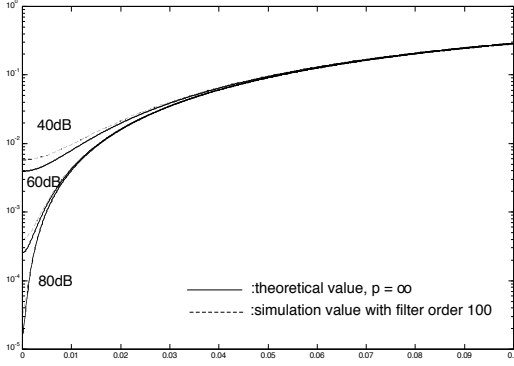


Fig. 2. MMSE vs. normalized frequency separation $\Delta f\sigma$ for $f_s = 5 f_{dm}$. Prediction range = $0.2/f_{dm}$.

From the linear prediction algorithm (3), the predicted fading signal $\hat{c}(f^2, n)$ is a zero-mean complex Gaussian random variable. Later in the paper, we employ different Gaussian estimates. Suppose $\alpha = \alpha(f^2, t)$ is the actual fading amplitude, and $\hat{\alpha}$ is the amplitude of a zero mean complex Gaussian estimate correlated with $c(f^2, t)$. Thus, the pdf of $\hat{\alpha}$ is $p(\hat{\alpha}) = (2\alpha/\hat{\Omega}) \exp(-\hat{\alpha}^2/\hat{\Omega})$, and the conditional probability density function (pdf) of α given $\hat{\alpha}$ is given by:

$$p(\alpha | \hat{\alpha}) = \frac{2\alpha}{(1-\rho)\hat{\Omega}} I_0\left(\frac{2\sqrt{\rho}\alpha\hat{\alpha}}{(1-\rho)\sqrt{\hat{\Omega}\hat{\Omega}}}\right) \exp\left(-\frac{1}{1-\rho}\left(\frac{\alpha^2}{\hat{\Omega}} + \frac{\rho\hat{\alpha}^2}{\hat{\Omega}}\right)\right) \quad (5)$$

where the correlation coefficient $\rho = \frac{\text{Cov}(\alpha^2, \hat{\alpha}^2)}{\sqrt{\text{Var}(\alpha^2)\text{Var}(\hat{\alpha}^2)}}$, $0 < \rho < 1$, $\hat{\Omega} = E\{\alpha^2\} = 1$, $\hat{\Omega} = E\{\hat{\alpha}^2\}$, and I_0 is the 0th order modified Bessel function. This conditional distribution will be used in the selection of modulation parameters in section 3.

If the channel statistics, such as the time and frequency domain correlation, are known, the optimum MMSE channel prediction can be employed as in (3). However, as the Doppler shifts in (1) vary, the model coefficients need to be updated continuously based on the observations. Since we are not able to observe the fading coefficients at frequency f^2 , we modify our approach as follows. First, we predict future channel coefficient $c(f^1, n)$ and then use the frequency correlation function to select the transmitter parameters at f^2 . The predicted CSI at f^1 are given by:

$$\hat{c}(f^1, n) = \sum_{j=1}^p g_j^*(n) c(f^1, n-j) \quad (6)$$

The coefficients $g_j(n)$ are determined using the Least Mean Square (LMS) adaptive tracking method $g_j(n+1) = g_j(n) + \mu \epsilon_n^* \hat{c}(f^1, n-j)$ where μ is the step size and $\epsilon_n = c(f^1, n) - \hat{c}(f^1, n)$. This adaptive tracking can be performed since the observations at frequency f^1 are available at the transmitter [7,9]. The recursive least square (RLS) algorithm can also be used to improve accuracy and reduce the observation interval [12,17]. The coefficients $\hat{c}(f^1, n)$ are interpolated to obtain predictions at the symbol rate at frequency f^1 [6].

Once $\hat{c}(f^1, n)$ is found, the adaptive modulation parameters for transmitting at f^2 at time n are selected. (Note that $\hat{c}(f^2, n)$ is not predicted directly). As explained in section 3, this procedure depends on the pdf of the $\alpha(f^2, n)$ given $\hat{\alpha}(f^1, n)$. If we assume perfect

CSI at frequency f^1 for sample n , this conditional pdf is determined by (5) with $\hat{\Omega} = \hat{\Omega} = 1$ and $\rho = 1/(1+(2\pi\Delta f\sigma)^2)$. In practice, this pdf is computed as in (5) using empirical estimates of $\hat{\Omega}$ and ρ and depends on the accuracy of prediction in (6). It can be shown that when the estimates $\hat{c}(f^1, n)$ are scaled so that $\hat{\Omega} = 1$, the performance of adaptive modulation is not affected. Hence throughout the paper, $\hat{\Omega}$ is normalized to 1 for simplicity, and the performance depends only on the parameter ρ . The adaptation of ρ to the variation of the rms delay spread is discussed in section 4.

3. ADAPTIVE TRANSMISSION AIDED BY LONG RANGE PREDICTION

In this paper, we employ variable rate and variable power square multilevel quadrature amplitude modulation (M-QAM) signal constellations due to their inherent spectral efficiency and ease of implementation [1,13]. First, consider fixed power discrete rate method. Given fixed transmitter power per symbol E_s (or average SNR level $\gamma = E_s/N_0$) and a target bit error rate (BER_{tg}), we adjust the modulation level M according to the instantaneous predicted channel gain in (6). Assume $\hat{\alpha}$ is the predicted channel gain at carrier f^1 and α is the actual gain at frequency f^2 . The BER bound, i.e. $BER_{M(i)}^*(\gamma, \hat{\alpha})$, can be obtained as [8] $BER_{M(i)}^*(\gamma, \hat{\alpha}) =$

$$\int_0^{\hat{\alpha}} BER_{M(i)}(\gamma x^2) p_{\hat{\alpha}}(x) dx, \text{ where } p_{\hat{\alpha}}(x) \text{ is described by (5) and}$$

$BER_{M(i)}$ is calculated from the BER bound of MQAM for the AWGN channel [1]: $BER_{M(i)}(\gamma) \leq 0.2 \exp(-1.5\gamma/(M(i)-1))$, $M(i) \geq 4$, $BER_{M(1)}(\gamma) = Q(\sqrt{2\gamma})$, where γ is the instantaneous signal-to-noise ratio per symbol. (In a related technique in [4], noiseless outdated CSI is assumed available at the transmitter, and the $BER_{M(i)}^*(\gamma, \hat{\alpha})$ is calculated based on a conditional Rician distribution of the current channel amplitude.)

The thresholds α_i are chosen as follows. When the predicted channel gain $\alpha_{i+1} \geq \alpha \geq \alpha_i$, $M(i)$ -QAM is employed, where $M(1) = 2$, $M(i) = 2^{2^{(i-1)}}$, $i = 2 \dots 4$, ($\alpha_5 = \infty$). The threshold α_i is the $\hat{\alpha}$ for which the bound $BER_{M(i)}^*(\gamma, \alpha_i) = BER_{tg}$, the target BER. The average BER of this fixed power discrete rate adaptive modulation is lower than the BER_{tg} since an upper bound is used and $BER_{M(i)}^*(\gamma, \hat{\alpha}) < BER_{tg}$ when $\hat{\alpha}$ does not take on a threshold value. Hence we utilize a power control policy to reduce the power consumption while maintaining the target BER. Once the modulation level M is decided for a particular $\hat{\alpha}$, a SNR level $\hat{\gamma}$ can be found by numerical search to maintain the target BER. Note that $\hat{\gamma}$ is less than or equal to γ . A similar power control method was proposed in [4]. The average bit per symbol \hat{R}_{ada} for both fixed and variable power methods is \hat{R}

$$\hat{R}_{ada} = \sum_{i=1}^4 \log_2 M_i \int_{\alpha_i}^{\alpha_{i+1}} p_{\hat{\alpha}}(x) dx. \quad \text{This rate also}$$

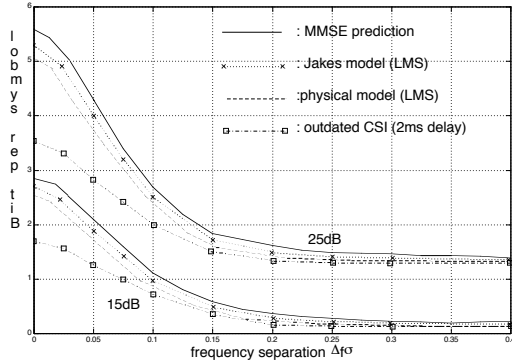


Fig.3. BPS vs. normalized frequency separation for different prediction techniques. $f_{dm} = 100\text{Hz}$. Prediction range is 2ms.

gives the spectral efficiency assuming the ideal Nyquist data pulse. For the power control method above, the average signal to

$$\text{noise ratio } \gamma_{\text{avg}} \text{ is } \gamma_{\text{avg}} = \int_0^{\hat{\gamma}} \gamma(x) p(\gamma(x)) dx.$$

4. SIMULATION RESULTS AND PERFORMANCE ANALYSIS

We use the Jakes model and our physical model to validate the performance of the continuous power discrete rate adaptive M-QAM aided by LRP. The maximum Doppler shift of 100 Hz is used in both models. The target BER = 10^{-3} . The fading signal is sampled at the rate of 500Hz for the LRP. The observation interval is 100 samples, the SNR in the observations is 80dB, the symbol rate is 25ksymbol/s, and the modulation-switching rate is set to the symbol rate. Interpolation is utilized to predict the channel coefficients at the symbol rate. The prediction range is 2ms. The physical model in [9,12] is extended to include multiple frequencies [17]. The reflectors are arranged to give an approximately exponential distribution of excess delay with the rms delay spread $\sigma \approx 1\mu\text{s}$.

In Fig. 3 we plot bits per symbol vs. normalized frequency separation $\Delta f\sigma$ for the ideal (non-adaptive) MMSE filter (3) and the robust method using the LMS algorithm (6) with the step size 0.005. The parameters in (5) are estimated during the observation interval for both data sets and are used throughout the transmission. For example, for $\Delta f = 0$, the estimated $\rho = 0.983$ for the Jakes model and $\rho = 0.965$ for the physical model. The bit rate loss is less than half a bit for non-stationary data generated by the physical model relative to the stationary case. We also investigated the BPS under the assumption that prediction is perfect at frequency f^1 . We observe that the performance of the robust algorithm is very close to this ideal case as well as to the performance of the ideal MMSE algorithm. This is consistent with the results in [8] where it is shown that when observations and the predicted samples are at the same frequency, performance of adaptive modulation aided by robust (adaptive) LRP closely approximates the ideal performance with perfect CSI. Hence the robust method is near-optimal and has the ability to adapt transmission parameters to the time-variant channel conditions. Moreover, for given σ , the theoretical parameter ρ in Section 2 can be utilized in the selection of thresholds

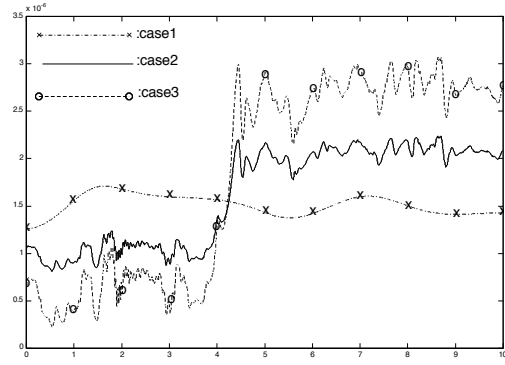


Fig. 4. The variation of the rms delay spread σ for typical (case 1) and challenging cases (case 2 and 3).

when robust prediction is used.

The performance of the adaptive modulation using the outdated CSI for the Rayleigh fading channel with the correlation function (2) is also shown in Fig.3. To alleviate the mismatch of the delayed and future CSI, a novel approach to calculate thresholds based on the delayed CSI was studied in [4]. A similar method is employed here. A single observation $c(f^1, n-1)$ is used instead of the estimate $\hat{c}(f^1, n)$ in (6) to compute the modulation parameters at frequency f^2 . We found that even very small delay causes significant loss of the bit rate for fast vehicle speeds when accurate long range prediction is not utilized. For example, for $\Delta f\sigma = 0$ and $\tau = 2\text{ms}$, the loss is 1 to 2 BPS. Thus, accurate LRP is required to achieve the bit rate gain of adaptive modulation for fast vehicle speeds and realistic delays.

Fig.3 also shows that adaptive modulation is primarily beneficial when the normalized frequency separation $\Delta f\sigma$ does not significantly exceed 0.1. For example, for $\Delta f\sigma = 0.1$, about 17 db is required to obtain 1 BPS for adaptive M-QAM as opposed to 24 db for non-adaptive signaling (BPSK). As $\Delta f\sigma$ approaches 0.4, the bit rate of adaptive modulation is very close to that of non-adaptive transmission. Hence the frequency separation and the multipath delay (or the coherence bandwidth) are the factors that determine the performance of the proposed adaptive modulation method. The typical values of σ are on the order of microseconds in outdoor mobile radio channel [11]. If $\Delta f\sigma = 0.1$ and $\sigma = 1\mu\text{sec}$, $\Delta f = 100\text{KHz}$. This means that two channels separated by 100KHz can still benefit from adaptive transmission.

Another practical consideration is the adaptation of the parameter ρ in (5) as a function of the variation of the rms delay spread σ . To investigate the limits on the speed of adaptation, we use the physical model to generate challenging and typical scenarios. In Fig.4, the variation of σ is shown for three cases where the reflectors are arranged to give an approximately exponential excess delay distribution. The rms delay spread σ is slowly varying for a typical case 1. In the challenging cases 2 and 3, σ varies rapidly due to shadowing of many reflectors by a nearby structure during a portion of the track. We investigate the performance of adaptive modulation on these channels during the T=1 sec interval when σ varies rapidly in cases 2 and 3 (3.5 to

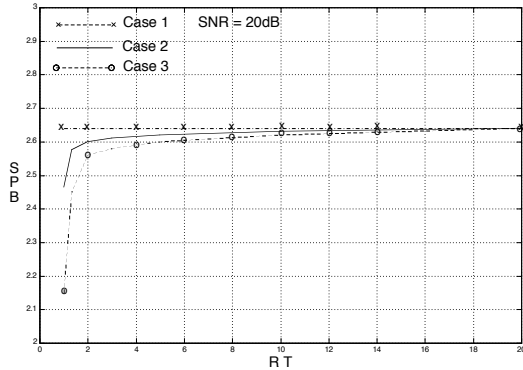


Fig. 5. BPS vs. normalized adaptation rate R,T . $SNR = 20dB$.
 $BER_{ig} = 10^{-3}$. $\Delta f = 50KHz$.

sec). The variation of the rms delay spread is approximately from 0.7 to 2.3 μs and 0.4 to 2.6 μs for case 2 and 3, respectively. The target BER is 10^{-3} and the power is adjusted to maintain the target BER to compensate for the mismatch of the rms delay. The parameter ρ is updated at the rate R , Hz. Fig. 5 illustrates the performance of adaptive modulation as a function of the adaptation rate R,T . When $R,T < 2$, there is significant performance loss for case 3 relative to the rms-invariant case 1. To improve performance, the correlation ρ needs to be tracked and updated more frequently. By analyzing datasets produced by the physical model, we concluded that the variation of the rms delay (and ρ) is typically slow and tracking of the correlation ρ does not result in significant additional computational and feedback load. The required rate of update of the parameter ρ is much slower even than the low sampling rate for predicting at frequency f^1 in (6). Thus, the proposed robust prediction method based on the observations at a different carrier is feasible, but infrequent update of the time-variant frequency correlation is required to satisfy the adaptive transmission performance criterion (e.g. the BER_{ig}).

In this paper, the assumption of the exponentially distributed propagation delay results in the relationship of the parameter ρ and the rms delay spread σ discussed in section 2. If the distribution of the propagation delay is different, this relationship will change. For example, for the uniform distribution, the coherence bandwidth and ρ are reduced for a given σ , and hence the performance of the prediction in the frequency domain and the bit rate are degraded relative to the exponentially distributed excess delay. Since we directly estimate the correlation ρ from the dataset, our algorithm is robust to the variation in the distribution of the excess delay.

5. CONCLUSION

A novel adaptive modulation method that uses predicted CSI of a different carrier was presented. The statistical model of the prediction accuracy distribution was created, and system performance was evaluated for various frequency separation values and rms delay spreads. We demonstrated that significant bit rate gains can be achieved relative to non-adaptive systems for realistic channel parameters, and that increased frequency separation and multipath delay limit the performance of adaptive transmission. We also used a novel physical model to investigate

the rate of adaptation to the variation of the rms delay spread. The results in this paper give valuable insights into designing adaptive transmission methods for correlated carriers and multicarrier systems.

6. REFERENCES

- [1] A.J. Goldsmith and S.G. Chua, "Variable-Rate Variable-power MQAM for Fading Channels", *IEEE Trans. Comm.*, vol. 45, No 10, Oct 1997, pp1218-1230.
- [2] A. J. Goldsmith and S. G. Chua, "Adaptive Coded Modulation for Fading Channels," *IEEE Trans. Commun.*, Vol. 46, No. 5, May 1998, pp. 595 - 601.
- [3] T. Ue, S. Sampei, N. Morinaga and K. Hamaguchi, "Symbol Rate and Modulation Level-Controlled Adaptive Modulation/TDMA/TDD System for High-Bit-Rate Wireless Data Transmission," *IEEE Trans. Veh. Technol.*, Vol. 47, No. 4, Nov. 1998, pp. 1134 - 1147.
- [4] D.L. Goeckel, "Adaptive Coding for Fading Channels using Outdated Channel Estimates," *IEEE Trans. Commun.*, Vol. 47, No. 6, June 1999, pp. 845-855.
- [5] K. Miya, O. Kato, K. Homma, T. Kitade, M. Hayashi, and T. Ue, "Wideband CDMA systems in TDD-mode operation for IMT-2000," *IEICE Trans. Commun.*, Vol. E81-B, July 1998, pp.1317-1326.
- [6] T. Eyceoz, A. Duel-Hallen, H. Hallen, "Deterministic Channel Modeling and Long Range Prediction of Fast Fading Mobile Radio Channels," *IEEE Commun. Lett.*, Vol. 2, No. 9, Sept. 1998, pp. 254 - 256.
- [7] T. Eyceoz, S. Hu, and A. Duel-Hallen, "Performance Analysis of Long Range Prediction for Fast Fading Channels," *Proc. of 33rd Annual Conf. on Inform. Sciences and Systems CISS'99*, March 1999, Vol. II, pp. 656 - 661.
- [8] S. Hu, A. Duel-Hallen, H. Hallen, "Long Range Prediction Makes Adaptive Modulation Feasible for Realistic Mobile Radio Channels," *Proc. of 34rd Annual Conf. on Inform. Sciences and Systems CISS'2000*, Vol. I, pp. WP4-7 ~ WP4-13, March 2000.
- [9] A. Duel-Hallen, S. Hu and H. Hallen, "Long Range Prediction of Fading Signals: Enabling Adaptive Transmission for Mobile Radio Channels," *IEEE Signal Processing Mag.*, Vol. 17, No. 3, pp. 62 - 75, May 2000.
- [10] W. C. Jakes, *Microwave Mobile Communications*. Wiley, New York, 1974.
- [11] T. S. Rappaport, *Wireless Communications: Principles and Practice*. Prentice-Hall, 1996.
- [12] H. Hallen, S. Hu, M. Lei and A. Duel-Hallen, "A Physical Model for Wireless Channels to Understand and Test Long Range Prediction of Flat Fading," *Proc. of WIRELESS 2001*, Calgary, Canada, July 9-11, 2001.
- [13] J. G. Proakis, *Digital Communications*. Third Edition, McGraw-Hill, 1995.
- [14] T. S. Yang, A. Duel-Hallen, "Adaptive Modulation Using Outdated Samples of Another Fading Channel," *Proc. IEEE Wireless Communications and Networking Conference*, vol. 1, pp. 477-481. Mar. 17-21, 2002.
- [15] T. S. Yang, "Performance Analysis of Adaptive Transmission at a Different Carrier Frequency and its Application aided by Long Range Prediction.", Ph.D. Thesis, NC State University, in preparation.
- [16] J. Salz, "Optimum Mean-Square Decision Feedback Equalization," *Bell Syst. Tech. J.*, Vol. 52, pp. 1341-1373, October, 1973.
- [17] H. Hallen, A. Duel-Hallen, S. Hu, T. S. Yang, M. Lei, "A Physical Model for Wireless Channels to Provide Insights for Long Range Prediction," *Proc. MILCOM'02*, Oct. 7-10, 2002.